Initiation of Roll Waves in Gas-Liquid Flows

Measurements of the effect of liquid viscosity on the initiation of roll waves in a horizontal gas-liquid flow are presented. These results are interpreted by an analysis based on the calculation of the growth of long wavelength disturbances.

PAOLO ANDREUSSI

Istituto di Chimica Industriale ed Applicata
University of Pisa
Pisa, Italy

and

J. C. ASALI and T. J. HANRATTY

Department of Chemical Engineering
University of Illinois
Urbana, IL 61801

SCOPE

A number of investigators have observed long wavelength disturbances or surges on liquid films, flowing concurrently with a gas. At low gas velocities, the initiation of these roll waves in a horizontal channel is more sensitive to changes of gas velocity than those of liquid velocity. At high gas velocities, the transition is insensitive to gas velocity and channel orientation, and occurs at an approximately constant liquid flow rate. A stability analysis by Hanratty and Hershman (1961), that uses a pseudosteady-state approximation to relate changes of the interfacial stress and the wall stress to changes of film height, is in approximate agreement with observed transitions at low gas velocities. However, the analysis indicates that at high enough gas velocities the film is unstable for all liquid flow rates.

The stability theory of Hershman and Hanratty is reexamined to determine forces that could be stabilizing thin liquid films and to improve the calculations for thick films. The results of this analysis are checked with new experimental results which determine the effect of changes of liquid viscosity on the critical liquid flow rate at high gas velocities.

CONCLUSIONS AND SIGNIFICANCE

The experiments show that the liquid Reynolds number at transition is weakly dependent on the product of the ratio of the liquid and gas viscosities and the square root of the ratio of the gas and liquid densities.

These results are consistent with an interpretation which views the transition as occurring when the destabilizing effects of inertia are larger than the stabilizing effects of the "out of phase" component of the interfacial stress (a maximum downstream of the crest). This "out of phase" component is assumed to occur because of relaxation from the pseudosteady-state mode.

An important application of these results is the interpretation and correlation of measurements of the entrainment of liquid by a high-speed gas flow. The critical film flow for the initiation of roll waves corresponds closely to the critical film flow below which no further entrainment occurs in gas-liquid annular flow. The prediction of the effect of changes of viscosity on entrainment depends critically on the prediction of its effect on this critical film flow.

INTRODUCTION

Long wavelength disturbances or flow surges on liquid films flowing concurrently with a gas have been observed by Kinney, Abramson and Sloop (1952), Knuth (1954), Hanratty and Engen (1957), Hanratty and Hershman (1961), Nedderman and Shearer (1963), Miya, Woodmansee and Hanratty (1971), Wurz (1977), Nencini and Andreussi (1982). These disturbances have the same appearance as turbulent roll waves flowing down an inclined plane (Iwasa, 1954; Ishihara et al., 1952; Mayer, 1957). The prediction of the conditions under which roll waves appear in gas-liquid flow has been of considerble interest since they affect transport in the film and since they can play an important role in the entrainment of liquid by the gas flow.

At low gas velocities the initiation of roll waves in a horizontal channel is more sensitive to changes of gas velocity than those of liquid velocity. At high gas velocities the transition is insensitive to gas velocity and channel orientation, and occurs at an approximately constant liquid flow rate. There appears to be some disagreement in the literature regarding the effect of liquid properties on this critical liquid flow rate. Ishii and Grolmes (1975) suggest that the transition occurs at a constant liquid Reynolds number at high gas velocities, but give no supporting theoretical arguments.

This paper presents new experimental results on the effect of changes of liquid viscosity on this transition in a horizontal channel, improves a previous theoretical analysis of this transition, and explores a possible theoretical interpretation of observations at high gas velocities.

Jeffreys (1975), Dressler (1949, 1952) and Iwasa (1954) have predicted the critical conditions for liquid flow down an inclined plane in the absence of a gas flow by examining the growth or decay of small disturbances on the liquid layer. Hanratty and Hershman (1961) have applied Jeffreys' analysis of small disturbances to gas-liquid flow in an enclosed horizontal rectangular channel. Reasonable agreement was obtained at small gas velocities. However, the analysis failed at high gas velocities.

The results obtained by Hanratty and Hershman show that gas-phase pressure variations and inertial effects caused by the presence of large wavelength disturbances are destabilizing influences on the film. When these effects are too large to be counterbalanced by gravity, roll waves can exist. For vertical flows or high gas velocities, the effect of gravity is zero or negligibly small, so the analysis provides no theoretical explanation of what stabilizes the film at low liquid flows. In fact, Hanratty and Hershman predict that at high enough gas velocities the film is unstable for all liquid flow rates.

At high gas velocities the liquid film is caused to move along the wall by the drag of the gas at the interface, so the modeling of the interfacial stress, τ_i, should play a central roll in any analysis. Hanratty and Hershman allowed τ_i to vary along the wave surface only because of changes in gas velocity. In an attempt to improve this theory, Miya (1970) argued that changes of the height of the wall layer will be accompanied by changes in the small wave structure and, therefore, the surface roughness. He modified the theory of Hanratty and Hershman by allowing the interfacial friction factor, f_i, as well as the gas velocity to change along the surface of the large disturbance wave. This analysis improves the prediction of the critical gas velocity at large liquid flows but fails to predict a critical liquid flow rate at large gas velocities.

The theoretical approach explored in this paper is an extension of the work of Miya. The chief difference is that it is assumed that the wave structure and the turbulence properties of the liquid do not adjust immediately to changes in the liquid height. Because of this, the interfacial friction factor and the fluid turbulence will not be maxima at the crest of the long wavelength disturbances. This gives rise to "out of phase" components of the interfacial stress and wall stress which can stabilize the liquid film at high gas velocities.

The experiments were carried out in the 10 m long horizontal 2.54 × 30.5 cm rectangular channel used by Miya et al. (1971). Liquid flowed along the bottom of the channel and air over the top of the liquid film. The viscosity of the liquid was varied by using glycerine-water solutions. An important result of the very extensive experiments reported in this paper is the finding that liquid viscosity has a much stronger effect on the transition than is suggested by the results of Woodmansee and Hanratty (1969) and of Knuth (1954, 1955).

MODEL EQUATIONS

Conservation of Mass and Momentum

The system considered is the concurrent flow of gas and liquid in an enclosed channel making an angle θ with the gravitational vector. As shown in Figure 1, the main direction of motion is along the Cartesian axis x. We also assume $y = 0$ at the wall of the channel. The gas exerts a shear stress, τ_i, at $y = h$ and the wall exerts a resisting stress, τ_w, on the liquid. By varying θ, we have the limiting cases: $\theta = 0$, vertical downward flow; $\theta = 90°$, horizontal flow; $\theta = 180°$, vertical upward flow. The heights of the liquid and gas spaces are h and $(B - h)$. Local average velocities in the liquid and the gas are defined as:

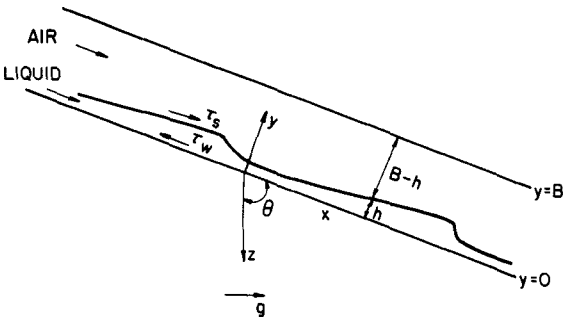

Figure 1. Diagram of system.

$$u_a h = \int_0^h u dy, \tag{1}$$

$$U_a(B - h) = \int_h^B U dy. \tag{2}$$

It is desired to determine the conditions under which wavelike disturbances will first appear at the interface because of an instability of the film to infinitesimal disturbances, i.e., neutral stability. To do this, we determine the conditions for which solutions of the linear momentum equations can be obtained for sinusoidal waves of steady form propagating with a velocity c in the positive x-direction. The waves being considered are broad-crested and the channel has a large enough aspect ratio that the equation for a two-dimensional field may be applied. The wave height to wavelength ratio is small enough that a shallow liquid assumption can be made, whereby the pressure is varying only because of changes of hydrostatic head

$$p = p_g + \rho_L g(h - y)\sin\theta - \sigma \frac{\partial^2 h}{\partial X^2}, \tag{3}$$

and the velocity variation in the y-direction is the same as would exist if a disturbance were not at the interface.

The flow field is described by integral forms of the equations of conservation of mass and momentum. These can be written in the following form in a coordinated system traveling with the wave velocity, $X = x - ct$, if the effects of surface tension, σ, in Eq. 3 are ignored:

$$h \frac{du_a}{dX} = (c - u_a)\frac{dh}{dX}, \tag{4}$$

$$\frac{d}{dX}(\Gamma h u_a^2) - c^2 \frac{dh}{dX} = \frac{1}{\rho_L}(\tau_i - \tau_w) + gh\cos\theta - \frac{h}{\rho_L}\left(\frac{dp_g}{dX} + g\rho_L \sin\theta \frac{dh}{dX}\right). \tag{5}$$

Here Γ is a shape factor defined as

$$\Gamma = \int_0^h u^2 dy / h u_a^2. \tag{6}$$

As suggested by Miya et al. (1971), the shallow fluid assumption can also be made for the gas phase since the wavelength of the disturbances are large compared to the dimensions of the gas space. The gas phase is fully turbulent so it is approximated by a plug flow of velocity U_a. The integral mass and momentum balances for the gas then give the following equation for the pressure gradient:

$$\frac{dp_g}{dX} = \rho_g \frac{1}{2}\frac{d}{dX}(U_a - c)^2 + \frac{\tau_i + \tau_B}{(B - h)}. \tag{7}$$

Growth of Small Disturbances

The propagation of small sinusoidal disturbances on a liquid film will be examined by using Eqs. 4 and 5. It is assumed, at liquid velocities exceeding the neutral stability condition, that an unstable sinusoidal disturbance eventually develops into the asymmetric roll wave that is observed in experiments. A small disturbance of

the film height, h' at neutral stability, is accompanied by disturbances in τ_w, τ_i, u_a, U_a, and p_g. These disturbances are represented by the equations

$$\frac{h'}{\hat{h}} = \frac{p_g'}{\hat{p}_g} = \frac{\tau_w'}{\hat{\tau}_w} = \frac{\tau_i'}{\hat{\tau}_i} = \frac{u_a'}{\hat{u}_a} = \frac{U_a'}{\hat{U}_a} = \exp\{i\alpha X\}, \tag{8}$$

where c, $\hat{h}$, and k are real and $\hat{p}_g, \hat{\tau}_i, \hat{\tau}_w, \hat{u}_a, \hat{U}_a$ can be complex. Thus, if only the real part of Eq. 8 is considered,

$$h' = \hat{h}\cos(\alpha X) \tag{9}$$

$$p_g' = \hat{p}_{g,R}\cos(\alpha X) - \hat{p}_{g,I}\sin(\alpha X) \tag{10}$$

$$\tau_i' = \hat{\tau}_{i,R}\cos(\alpha X) - \hat{\tau}_{i,I}\sin(\alpha X) \tag{11}$$

$$\tau_w' = \hat{\tau}_{w,R}\cos(\alpha X) - \hat{\tau}_{w,I}\sin(\alpha X) \tag{12}$$

The amplitudes $\hat{\tau}_{i,R}, \hat{p}_{g,R}, \hat{\tau}_{w,R}$ are the components of τ_i', p_g', τ_w' in phase with the wave height; the amplitudes $\hat{\tau}_{i,I}, \hat{p}_{g,I}, \hat{\tau}_{w,I}$ are the components, in phase with the wave slope. It is noted that $\hat{p}_{g,R}$ is negative and that $\hat{\tau}_{i,R}$ and $\hat{\tau}_{w,R}$ are positive. A positive value of $\hat{p}_{i,I}$ causes the minimum pressure to be upstream of the wave crest. Positive values of $\hat{\tau}_{i,I}$ and $\hat{\tau}_{w,I}$ indicate that the maxima of the interfacial drag and of the wall resistance are upstream of the wave crest.

For small distrubances, Eqs. 5 and 6 can be linearized around some steady conditions. The following two equations are then derived for neutral stability:

$$\left(c^2 + \bar{u}_a^2\bar{\Gamma} - 2\bar{u}_a\bar{\Gamma}c - \bar{h}\bar{u}_a^2\frac{\hat{\Gamma}}{\hat{h}}\right)\rho_L\alpha = \frac{\hat{\tau}_{i,I}}{\hat{h}} - \frac{\hat{\tau}_{w,I}}{\hat{h}} - \bar{h}\alpha\left(\frac{\hat{p}_{g,R}}{\hat{h}} + g\rho_L\sin\theta\right), \tag{13}$$

$$\frac{\hat{\tau}_{i,R}}{\hat{h}} - \frac{\hat{\tau}_{w,R}}{\hat{h}} + g\rho_L\cos\theta - \left(\frac{d\bar{p}}{dx}\right) + \bar{h}\,\alpha\frac{\hat{p}_{g,I}}{\hat{h}} = 0. \tag{14}$$

In these equations the barred quantities are the values for the undisturbed flow. Pressure variations over the wave can be determined from Eq. 7 as:

$$\frac{\hat{p}_{g,R}}{\hat{h}} = \frac{\rho_g}{B-\bar{h}}\left[-(\bar{U}_a - c)^2 - \frac{1}{\alpha\rho_g}\left(\frac{\hat{\tau}_{i,I}}{\hat{h}} + \frac{\hat{\tau}_{B,I}}{\hat{h}}\right)\right], \tag{15}$$

$$\frac{\hat{p}_{g,I}}{\hat{h}} = \frac{1}{\alpha}\frac{1}{(B-\bar{h})}\left[\left(\frac{\hat{\tau}_{i,R}}{\hat{h}} + \frac{\hat{\tau}_{B,R}}{\hat{h}}\right) - \frac{d\bar{p}_g}{dX}\right]. \tag{16}$$

Finally, the mass balance equations for the liquid and the gas are given by

$$\frac{\hat{u}_a}{\hat{h}} = \frac{c-\bar{u}_a}{\bar{h}}, \tag{17}$$

$$\frac{\hat{U}_a}{\hat{h}} = \frac{\bar{U}_a - c}{B-\bar{h}}. \tag{18}$$

Interpretation of the Neutral Stability Equations

In Eq. 14 the wall shear stress amplitude, $\hat{\tau}_{w,R}$, can be related to the amplitude of the disturbances in the liquid flow, $\hat{u}_a$, and, therefore, to the wave velocity, c, through Eq. 17. Consequently, Eq. 14 may be viewed as the equation defining c under neutral stability conditions. This velocity is the kinematic wave velocity defined by Lighthill and Whitman (1955).

Equation 13 defines the flow condition at the roll wave transition. The term $-\rho_L g\bar{h}\alpha\sin\theta$ is negative and represents the stabilizing influence of gravity. The second two terms on the right side of Eq. 15 are usually small so $\hat{p}_{g,R}$ is a negative number. Consequently $-\bar{h}\alpha\hat{p}_{g,R}/\hat{h}$ is positive and destabilizing. The inertia terms on the left side of Eq. 13 are usually negative and, therefore, destabilizing.

For large liquid flows, or large $\bar{h}$, the terms $\hat{\tau}_{i,I}/\hat{h}$ and $\hat{\tau}_{w,I}/\hat{h}$ are small compared to the other terms on the right side of Eq. 13. Instability then occurs when the destabilizing effects of inertia and of $\hat{p}_{g,R}$ are larger than the stailizing influence of gravity. Since the magnitude of $\hat{p}_{g,R}$ increases with increasing gas velocity, this type of consideration leads to the prediction of a critical gas velocity for the initiation. Consequently, the neglect of the $\hat{\tau}_{i,I}$ and $\hat{\tau}_{w,I}$ terms predicts an upper bound for the critical gas velocity when inertia effects vanish, given by the equation

$$\frac{\hat{p}_{g,R}}{\hat{h}} = \rho_L g\sin\theta. \tag{19}$$

For small liquid flows a negative $\hat{\tau}_{i,I}\hat{h}$ or a positive $\hat{\tau}_{w,I}\hat{h}$ can be stabilizing. Thus, the existence of stable liquid films at gas velocities larger than those given by Eq. 19 can be explained from linear stability theory, only if the interfacial stress has a maximum downstream of the crest or if the wall stress has a maximum upstream of the crest.

It is clear that the evaluation of the wave-induced variation of the surface and wall stresses is the central problem in the analysis of the stability of the liquid film to small disturbances.

EVALUATION OF THE INTERFACIAL AND WALL SHEAR STRESSES

Pseudosteady-State approximation for τ_w

A relation for τ_w can be obtained by making a pseudosteady-state assumption whereby the dependence of τ_w on u_a and h is the same as for steady flow. In many instances, flow in the undisturbed film may be represented by a turbulent relation,

$$\frac{u}{u_c^*} = f\left(\frac{yu_c^*}{\nu_L}\right), \tag{20}$$

$$u_c^* = (\tau_c/\rho_L)^{1/2}, \tag{21}$$

$$\tau_c = \frac{2}{3}\tau_w + \frac{1}{3}\tau_i. \tag{22}$$

The integration of Eq. 20 from 0 to h^+ yields the following result (Henstock and Hanratty, 1976):

$$\frac{hu_c^*}{\nu_L} = g(Re_L) \tag{23}$$

$$g(Re_L) = [(1.414\,Re_L^{0.5})^{2.5} + (0.132Re_L^{0.9})^{2.5}]^{0.4} \tag{24}$$

where $Re_L = hu_a/\nu_L$ is the liquid film Reynolds number. As shown by Hanratty and Hershman (1961), this can be rearranged in the form

$$\tau_w = \frac{2\mu_L u_a}{h}A(Re_L) - \frac{1}{3}h\tilde{P}, \tag{25}$$

with

$$A(Re_L) = g^2(Re_L)/2Re_L, \tag{26}$$

$$\tilde{P} = \frac{dp}{dx} - \rho_L g\cos\theta, \tag{27a}$$

$$= (\tau_i - \tau_w)/h. \tag{27b}$$

For the case of a thin laminar film $A(Re) = 1$.

It is assumed that Eq. 25 holds both for the disturbed and undisturbed flow, with $\tilde{P}$ given by Eq. 27b. Consequently, the variables can be replaced by the sum of a time-averaged and a fluctuating component. The subtraction of the time-averaged equation, the neglect of quadratic terms in the fluctuating quantities, and the use of conservation of mass to relate u_a' to h' give the following equation for τ_w':

$$\tau_w' = \frac{3\mu_L\bar{u}_a\bar{A}(\bar{Re}_L)}{\bar{h}}\left[\left(\frac{c}{\bar{u}_a} - 2\right)\frac{h'}{\bar{h}} + \frac{d\bar{A}}{d\bar{Re}_L}\frac{Re'}{\bar{A}}\right] - \frac{1}{2}\tau_i'. \tag{28}$$

From conservation of mass,

$$Re_L' = \bar{Re}_L\frac{c}{\bar{u}_a}\frac{h'}{\bar{h}} \tag{29}$$

The substitution of Eqs. 29 and 8 into Eq. 28 gives

$$\hat{\tau}_w = \frac{3\mu_L \bar{u}_a A(\overline{Re}_L)}{\bar{h}^2}\left[\frac{c}{\bar{u}_a} - 2 + \frac{c}{\bar{u}_a}\frac{\overline{Re}_L}{\bar{A}}\frac{d\bar{A}}{d\overline{Re}_L}\right] - \frac{1}{2}\hat{t}_i \quad (30)$$

Pseudosteady-State Approximations for τ_i

The interfacial stress for flow over a wavy film can be expressed as

$$\tau_i = \frac{1}{2} f_i \rho_g (U_a - c)^2 \quad (31)$$

From Eq. 31 it follows that the pertubation of τ_i due to the presence of a small disturbance is

$$\frac{\tau_i'}{\bar{\tau}_i} = \frac{f_i'}{\bar{f}_i} + 2\left(\frac{U_a'}{\bar{U}_a - c}\right), \quad (32)$$

where gas compressibility effects have been neglected. Hanratty and Hershman (1961) assumed $f_i' = 0$. Following Miya et al. (1970), we assume that f_i is a function of the perturbation of the gas and liquid flows by the presence of a disturbance at the interface:

$$\frac{f_i'}{\bar{f}_i} = \frac{1}{\bar{f}_i}\left(\frac{\partial \bar{f}_i}{\partial \overline{Re}_L} Re_L' + \frac{\partial \bar{f}_i}{\partial \overline{Re}_G} Re_G'\right) \quad (33)$$

From the equation of conservation of mass for the gas if $U_a/c \gg 1$ and $Re_G' = 0$

$$\frac{U_a'}{\bar{U}_a - c} = \frac{h'}{B - \bar{h}}. \quad (34)$$

Therefore Eq. 32 can be simplified to

$$\frac{\tau_i'}{\bar{\tau}_i} = 2\frac{h'}{B - \bar{h}} + \frac{\overline{Re}_L}{\bar{f}_i}\left(\frac{\partial \bar{f}_i}{\partial \overline{Re}_L}\right)\frac{c}{\bar{u}_a}\frac{h'}{\bar{h}}, \quad (35)$$

Substituting Eq. 8 into Eq. 35 yields the following relations for the amplitude of the perturbation of the fluctuating interfacial stress:

$$\frac{\hat{\tau}_{i,R}}{\bar{\tau}_i} = 2\frac{\hat{h}}{B - \bar{h}} + \frac{\overline{Re}_L}{\bar{f}_i}\left(\frac{\partial \bar{f}_i}{\partial \overline{Re}_L}\right)\frac{c}{\bar{u}_a}\frac{\hat{h}}{\bar{h}}, \quad (36)$$

$$\frac{\hat{\tau}_{i,I}}{\bar{\tau}_i} = 0. \quad (37)$$

The interfacial stress at the top wall, τ_B, also enters the stability condition (Eq. 19) through the $\hat{p}_{g,R}$ term. We can approximate the amplitude of the perturbation of this stress by

$$\frac{\hat{\tau}_{B,R}}{\hat{\tau}_{i,R}} = \frac{\bar{\tau}_B}{\bar{\tau}_i} = \phi, \quad (38)$$

$$\frac{\hat{\tau}_{B,I}}{\hat{h}} = 0. \quad (39)$$

The influence of $\hat{\tau}_{B,R}$ on the calculations to be presented later is found to be small.

Relaxation Effects in Approximating τ_i and τ_w

The principal assumptions in deriving Eqs. 30, 36 and 37 are that the dependencies of τ_i and τ_w on h, u_a and U_a are same as for a steady flow and that h^+ is a function of Re_L. Note that at large gas velocities, these equations predict that $\hat{\tau}_{i,I} = 0$ and $\hat{\tau}_{w,I} = 0$. These terms provide no stabilization for thin films and cannot account for the observed critical liquid flow rate. Consequently, we have explored simple empirical methods to relax the pseudosteady-state assumption.

The dependency of f_i on Re_L in Eq. 33 comes about because the wave roughness of the interface increases with increasing liquid flow rate or film height. It does not seem likely that the roughness adjusts immediately to changes in the height. Consequently, we assume there is a lag in the change of τ_i with a change in Re_L and that we can evaluate an effective Reynolds number, $Re_{L,e}$, at which τ_i should be calculated by means of the rate equation

$$\frac{d}{dx}(Re_{L,e}) = \frac{Re_L - Re_{L,e}}{m_{L,i}}, \quad (40)$$

where $m_{L,i}$ is a lag parameter. For a spatial variation of the flow field given by Eq. 8, we obtain from Eq. 40

$$Re_{L,e}' = \frac{Re_L'}{1 + \alpha^2 m_{L,i}^2}(1 - i\alpha m_L). \quad (41)$$

In this equation, we can assume that $\alpha^2 m_{L,i}^2 \ll 1$ as the disturbance waves have a very large wavelength and we do not anticipate that $m_{L,i}$ will be large.

$$Re_{L,e}' = Re_L'(1 - i\alpha m_{L,i}). \quad (42)$$

The lag parameter $m_{L,i}$ which determines the phase shift between τ_i and h' is expected to depend on the amplitude or wavelength of the capillary waves which cover the gas-liquid interface. It has the dimensions of length. We assume that for thin films the amplitude and wavelength of the small waves scale as the film thickness so we use the following simple expression for $m_{L,i}$:

$$m_{L,i} = \gamma_i \bar{h}, \quad (43)$$

where γ_i is a constant.

If Eqs. 42 and 29 are substituted for Re_L' in Eq. 33, the following equation for $\hat{\tau}_{i,I}$ is derived:

$$\frac{\hat{\tau}_{i,I}}{\bar{\tau}_i} = -\alpha\gamma_i \bar{h}\frac{\overline{Re}_L}{\bar{f}_i}\left(\frac{\partial \bar{f}_i}{\partial \overline{Re}_L}\right)\frac{c_R}{\bar{u}_a}\frac{\hat{h}}{\bar{h}} \quad (44)$$

The equation for $\hat{\tau}_{i,R}$ remains the same as Eq. 36.

A similar approach may be taken to derive an empirical equation for the relaxation of the expression for τ_w' from that derived using a pseudo-steady state assumption. The roll waves have a velocity greater than the fluid velocity at the interface. This means that fluid of relatively low turbulence is entrained at the front of the waves and that this fluid becomes more turbulent as the height of the liquid above it increases. It could be argued that because the fluid does not adjust immediately to the surroundings there is a tendency for the increase in the intensity of turbulent transport to lag the increase in film height. This would influence the wall drag to be a maximum on the upstream side of the wave.

CALCULATION OF THE TRANSITION

Neutral stability conditions can now be derived by the substitution of Eqs. 15, 16, 30, 36, and 44, into Eqs. 13 and 14. The resulting equations take the following forms:

$$\frac{c}{\bar{u}_a} = \frac{2 - \frac{1}{3}\frac{P}{A} - \frac{H}{3}\frac{P_1}{A} + \frac{2}{3}TH\left[\frac{3}{2} + H(1 + \phi)\right]}{1 + \frac{\overline{Re}L}{A}\frac{dA}{d\overline{Re}_L} - \frac{1}{3}T\frac{\overline{Re}_L}{\bar{f}_i}\left(\frac{d\bar{f}_i}{d\overline{Re}_L}\right)\left(\frac{3}{2} + H\right)} \quad (45)$$

$$c^2 - 2c\bar{u}_a\left(\bar{\Gamma} + \frac{d\bar{\Gamma}}{d\overline{Re}_L}\frac{\overline{Re}_L}{2}\right) + \bar{\Gamma}\bar{u}_a^2 = g\bar{h}\sin\theta - \frac{\rho_g}{\rho_L}H(\bar{U}_a - c)^2 + \frac{3}{2}\gamma_i\frac{\bar{\tau}_i}{\rho_L}\frac{\overline{Re}_L}{\bar{f}_i}\left(\frac{\partial f_i}{\partial \overline{Re}_L}\right)\frac{c}{\bar{u}_a}\left(1 + \frac{2}{3}H\right) \quad (46)$$

with

$$T = \bar{\tau}_i \Big/ \frac{A\mu_L \bar{u}_a}{\bar{h}} = 2\frac{\bar{\tau}_i}{\bar{\tau}_c} \quad P = \bar{P}\bar{h}^2/\mu_L\bar{u}_a.$$

$$H = \bar{h}/(B - \bar{h}) \quad P_1 = \frac{d\bar{p}}{dx}\bar{h}^2/\mu_L\bar{u}_a$$

For horizontal flows, $P = P_1$.

It is to be noted that

$$\frac{d\overline{Re}_L}{dh_L^+} = \frac{d}{dh_L^+}\int_0^{h_L^+} u^+(y^+)dy^+ = u_i^+ \quad (47)$$

Therefore, from Eqs. 23 and 26

$$\frac{\overline{Re}_L}{A}\frac{dA}{d\overline{Re}_L} = \frac{\overline{Re}_L}{A}\frac{dA}{dh_L^+}\frac{dh_L^+}{d\overline{Re}_L} = 2\frac{\bar{u}_a}{\bar{u}_i} - 1. \quad (48)$$

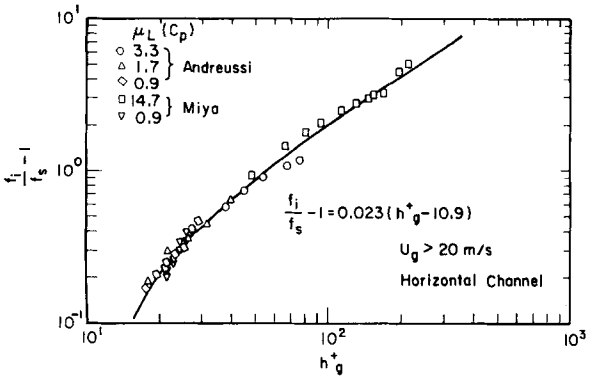

Figure 2. Friction factor measurements for gas velocities greater than 20 m/s.

From measurements of pressure drop by Andreussi and by Miya shown in Figure 2, the following equation has been derived for f_i prior to the transition to roll waves at high gas velocities:

$$\frac{f_i}{f_s} - 1 = 0.023(h_g^+ - 10.9), \tag{49}$$

where f_s is the friction factor for single-phase flow,

$$f_s = 0.046 Re_g^{-0.2} \tag{50}$$

and $h_g^+ = hu_g^*/\nu_g, u_g^* = (\tau_i/\rho_g)^{1/2}$. This can be written in the following form, valid for both high and low gas velocities at the transition

$$f_i = f_s(\delta + \beta h_g^+), \tag{51}$$

with δ and β functions of gas Reynolds number. In Eq. 49, we can express h_g^+ as a function of Re_L and of τ_i/τ_c through the dimensionless height, h_L^+. We then obtain

$$h_g^+ = h_L^+(Re_L)\frac{\nu_L}{\nu_g}\left(\frac{\tau_i}{\tau_c}\frac{\rho_L}{\rho_g}\right)^{1/2}. \tag{52}$$

Now, making use of the assumption that $h_L^+ = h_L^+(Re_L)$, it follows that

$$\frac{\overline{Re}_L}{\bar{f}_i}\left(\frac{\partial \bar{f}_i}{\partial \overline{Re}_L}\right) = \frac{\overline{Re}_L}{\bar{f}_i}\left(\frac{\partial f_i}{\partial h_L^+}\right)\frac{dh_L^+}{d\overline{Re}_L}. \tag{53}$$

Using Eqs. 49, 52 and 47,

$$\frac{\overline{Re}_L}{\bar{f}_i}\left(\frac{\partial \bar{f}_i}{\partial \overline{Re}_L}\right) = \frac{\bar{u}_a}{\bar{u}_i}\left(\frac{\beta h_g^+}{\delta + \beta h_g^+}\right), \tag{54}$$

From Eq. 54

$$\frac{T}{2}\frac{\overline{Re}_L}{\bar{f}_i}\frac{\partial \bar{f}_i}{\partial \overline{Re}_L} = \frac{\bar{u}_a}{\bar{u}_i}\left(\frac{\beta h_g^+}{\delta + \beta h_g^+}\right)\frac{\bar{\tau}_i}{\bar{\tau}_c} \tag{55}$$

If Eqs. 48 and 55 are substituted into Eqs. 45 and 46, the following equation is obtained for c:

$$\frac{c}{\bar{u}_i} = \frac{1 - \frac{1}{6}\frac{P}{A}(1+H) + \frac{2}{3}\frac{\tau_i}{\tau_c}H\left[\frac{3}{2} + H(1+\phi)\right]}{1 - \frac{1}{3}\frac{\tau_i}{\tau_c}\left(\frac{3}{2} + H\right)A_f} \tag{56}$$

$$A_f = \beta h_L^+(Re_L)\frac{\nu}{\nu_g}\left(\frac{\tau_i \rho_L}{\tau_c \rho_g}\right)^{1/2} \Big/ \delta + \beta h^+(Re_L)\frac{\nu_L}{\nu_g}\left(\frac{\tau_i \rho_L}{\tau_c \rho_g}\right)^{1/2} \tag{57}$$

Since

$$\frac{\overline{Re}_L}{\bar{f}_i}\frac{\partial \bar{f}_i}{\partial \overline{Re}_L} = \frac{\bar{u}_a}{\bar{u}_i}A_f, \tag{58}$$

the following neutral stability condition is obtained from Eq. 46

$$\frac{\tau_c}{\tau_i}\bar{u}_i^{+2}\left[\left(\frac{c}{\bar{u}_i}\right)^2 - 2\left(\frac{c}{\bar{u}_i}\right)\left(\frac{\bar{u}_a}{\bar{u}_i}\right)\left(\bar{\Gamma} + \frac{d\bar{\Gamma}}{d\overline{Re}_L}\frac{\overline{Re}_L}{2}\right) + \bar{\Gamma}\left(\frac{\bar{u}_a}{\bar{u}_i}\right)^2\right]$$

$$= \sin\theta\frac{\rho_L g\bar{h}}{\bar{\tau}} - \frac{(\bar{U}_a - c)^2\rho_g}{\bar{\tau}_i}H + \frac{3}{2}\gamma_i A_f\frac{c}{\bar{u}_i}\left(1 - \frac{2}{3}H\right) \tag{59}$$

From Eqs. 20 and 6, it is noted that

$$u_i^+ = f(h_L^+) \tag{60}$$

$$\frac{u_a}{u_i} = \frac{Re_L}{h_L^+ f(h_L^+)} \tag{61}$$

$$\Gamma = \frac{h_L^+}{Re_L^2}\int_0^{h_L^{+2}} f^2(y^+)dy^+ \tag{62}$$

The function $f(y^+)$ in Eqs. 60, 61 and 62 is evaluated from the van Driest mixing length equation (Hanratty and Henstock, 1976) using a van Driest constant of $A = 26$ and a von Karman constant of $\kappa = 0.6$. The reason for using $\kappa = 0.6$, rather than the usual $\kappa = 0.4$, is that this choice seems to give a better description of the film height measurements made by Miya (1970) in a horizontal channel.

Hanratty and Hershman (1961) used Eqs. 56 and 59 to predict the transition for thick films with $\partial \bar{f}_i/\partial \overline{Re}_L = 0$ and $\gamma_i = 0$. The left side of Eq. 59 is the destabilizing influence of inertia. Transition is predicted when the destabilizing effect of inertia and of pressure variations in phase with the wave height (second term on right side) overcome the stabilizing influence of gravity (first term on right side). Their assumption of $\partial f_i/\partial \overline{Re}_L = 0$, or $A_f = 0$, caused them to predict too small a value of $c/\bar{u}_i$, and therefore, to underestimate inertial effects. Their assumption of $\gamma_i = 0$ eliminated an important possible stabilizing effect for very thin films.

CALCULATION OF THE TRANSITION FOR HIGH GAS VELOCITIES

For high gas velocities, the film is quite thin and H is a small quantity, so that terms containing this quantity can be ignored. Likewise, under the conditions where the roll wave transition occurs $\bar{h}$ is so small that $\tau_i \simeq \tau_c$ and the stabilizing influence of gravity and the destabilizing influence of wave-induced pressure variations can be ignored. Neutral stability conditions (Eqs. 56 and 59), therefore, simplify to

$$\frac{c}{\bar{u}_i} = \frac{1}{1 - A_f/2}, \tag{63}$$

$$\bar{u}_i^{+2}\left[\left(\frac{c}{\bar{u}_i}\right)^2 - 2\frac{c}{\bar{u}_i}\left(\frac{\bar{u}_a}{\bar{u}_i}\right)\left(\bar{\Gamma} + \frac{d\bar{\Gamma}}{d\overline{RE}_L}\frac{\overline{RE}_L}{2}\right) + \bar{\Gamma}\left(\frac{\bar{u}_a}{\bar{u}_i}\right)^2\right] = \frac{3}{2}\gamma_i A_f\frac{c}{\bar{u}_i}, \tag{64}$$

with A_f defined by Eq. 57. For high gas velocities, the friction factor relation (Eq. 51) with $\delta = 0.75$, $\beta = 0.023$ and $\tau_i \simeq \tau_c$ was used. It follows that A_f is a function of $\overline{Re}_L$ and fluid property group $\mu_L\rho_g^{1/2}/\mu_g\rho_L^{1/2}$, and independent of gas Reynolds number.

From Eq. 57, it is seen that A_f is positive and less than unity. It follows from Eq. 63 that the wave velocity is larger than $\bar{u}_i$. From Eqs. 60, 61 and 62, and the relation $c > \bar{u}_i$, it is found that the inertia terms on the left side of Eq. 64 are destabilizing. Transition at high gas velocities occurs where the destabilizing influence of inertia is larger than the stabilizing influence of wave-induced shear stress variations at the interface which are out of phase with the wave height.

Since from Eqs. 23 and 24, h^+ is a function of Re_L, it follows from eqs. 60, 61, 62 and 63 that the inertia terms in Eq. 64 are a function of $\overline{Re}_L$ and A_f, defined by Eq. 57. Consequently, if the relaxation parameter γ_i is a constant, the above analysis predicts that the critical liquid Reynolds number is independent of gas Reynolds number and is a function of fluid properties through the dimensionless group $\mu_L\rho_g^{1/2}/\mu_g\rho_L^{1/2}$. Plots of this function for different values of γ_i are given in Figure 3.

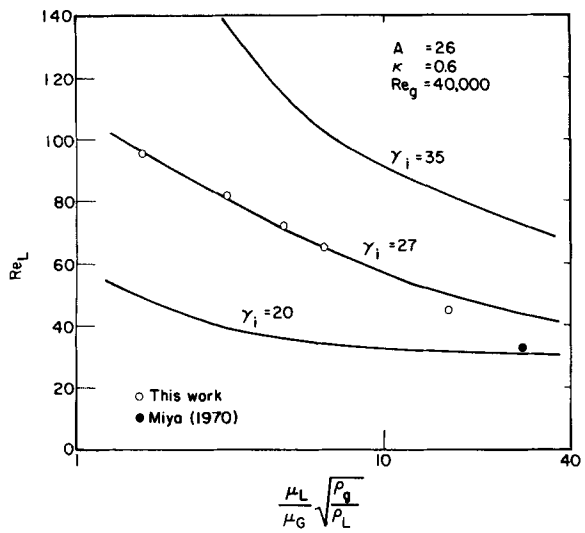

Figure 3. Effect of liquid viscosity on the transition Reynolds number at a gas Reynolds number of 40,000.

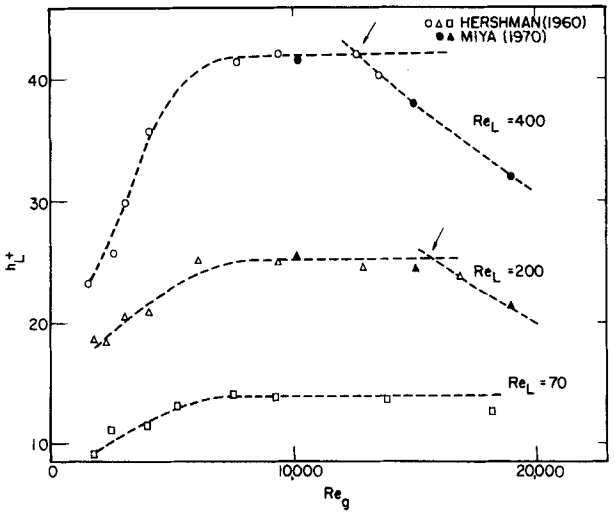

Figure 4. Measurements of the variation of the dimensionless height h_L^+ with liquid Reynolds number. The arrow indicates the transition to roll waves.

EXPERIMENTAL RESULTS

Experimental Observations

The different flow regimens encountered in the horizontal channel used for the experiments have been described by Woomansee (1969), Hanratty and Engen (1957), and Miya (1970). In this research a more careful examination was made of the effect of liquid viscosity on the transition at high gas velocities. The main result has been that above a gas Reynolds number of 20,000, the transition to roll waves is approximately independent of the gas velocity. However, data taken at very high gas velocities (40–70 m/s) could have been affected by evaporation of the liquid, as the gas stream was not saturated before the inlet. We, therefore, do not consider these data in the analysis.

The transition to roll waves was determined visually. It was sharp and clear at high gas, low liquid flow rates; at low gas, high liquid flows. The characteristics of the roll waves change with gas velocity. At low gas velocities, they are bidimensional and it is possible to observe a pebbly crest which advances at a constant velocity and precedes a smooth bidimensional patch about 2 cm long. At high gas velocities, roll waves, at their first appearance, do not extend across the entire width of the chanel, and the crest appears as an irregular line which advances at different velocities at different locations.

With increasing liquid viscosity, many of the characteristics of the interface changed and the transition to roll waves was less pronounced. For low viscosity fluids, the interface of the film prior to the transition has a pebbly appearance because it is covered by three-dimensional capillary wavelets. At higher liquid viscosities (μ_L = 0.086 g/cm·s), the wavelength of the ripples increases and the ripples tend to be two-dimensional up to the transition to roll waves. Miya (1970) describes the transition for μ_L = 0.147 g/cm·s and Re_g = 24,000 as occurring between a "laminar roll wave" regime to a "turbulent roll wave" regime. According to our observations, the two regimes differ because the "turbulent roll waves" have a higher velocity, are more coherent, and have a larger variability in their period than the "laminar roll waves."

Flow Characteristics of the Film

Experiments performed by Hershman (1960) for gas Reynolds numbers above 5,000–7,000 show the film flow appears to be turbulent even for very small values of the liquid-phase Reynolds number. The character of the flow is also revealed by a close examination of film thickness measurements by Hershman (1960) and Miya (1970). Figure 4 presents the results on the variation of h_L^+ with gas Reynolds number for three different liquid Reynolds numbers.

At low gas flows ($Re_g \to 0$), the relation between h_L^+ and Re_L is described reasonably well by the laminar flow equation. It is noted that h_L^+ increases with increasing Re_g until at high enough values it reaches a plateau whose value is given by a turbulent flow relation similar to Eq. 24. The transition to roll waves is marked by a decrease in h_L^+ with further increase in Re_g.

For the stability analysis, we are only interested in the behavior of the film prior to the transition to roll waves. That is, we are interested only in the plateau region shown in Figure 4. Measurements of this type are shown in Figure 5. Measured values of h^+ appear to be lower than predicted by Eq. 24 at low Re_L. This can be attributed to the nonlinear relation between Re_L and h_L^+ in this range, for which rippling or nonuniform liquid flows may cause a thinner film than predicted by the laminar flow relation. For higher Re_L, the values of h_L^+ are higher than predicted. This has also been noted by Miya et al. (1971), who proposed the use of a different value of the von Karman constant in order to explain the results.

Observed Conditions for Transition

Observations of the conditions for the initiation of roll waves are shown in Figure 6 for two liquid viscosities. These results clearly show that at large gas velocities the transition is approximately independent of gas flow. For water (μ_L = 0.009 g/cm·s) the critical condition at large gas velocities is given by $Re_L \simeq 95$. An increase of the viscosity nearly threefold has a weak influence on the critical condition, $Re_L \simeq 70$.

A more detailed study of the influence of liquid viscosity on the transition at high gas velocities is given in Figure 3. This shows that the critical liquid Reynolds number decreases monotonically with increasing $\mu_L \rho_g^{1/2} / \mu_G \rho_L^{1/2}$.

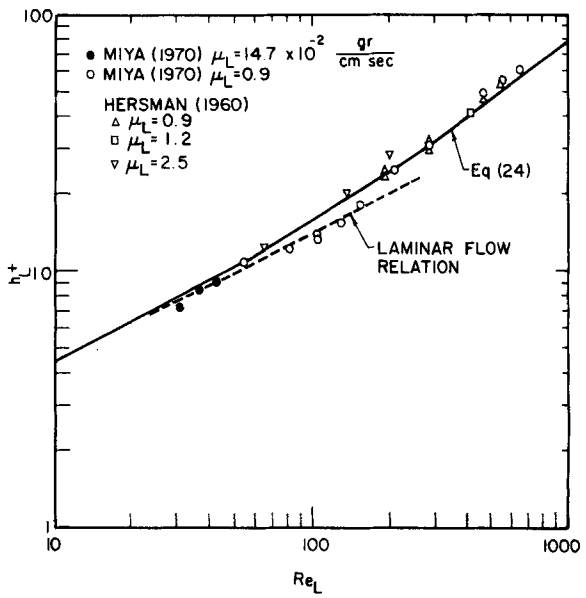

Figure 5. Height measurements of the liquid film just prior to the transition.

TABLE 1. MEASURED VALUES OF COEFFICIENT APPEARING IN EQ. 51

	Miya		Andreussi	
Reg	δ	β	δ^*	β^*
10,000	1.02	3.57×10^{-3}		
14,000	1.1	5.25×10^{-3}		
17,000	0.82	1.2×10^{-2}		
24,000	0.63	2.45×10^{-2}	0.75	2.3×10^{-2}
30,000	0.6	3.07×10^{-2}	0.75	2.3×10^{-2}
37,000	0.57	3.57×10^{-2}	0.75	2.3×10^{-2}
47,000	0.84	2.67×10^{-2}	0.75	2.3×10^{-2}

* δ and β were calculated by Eq. 49.

COMPARISON WITH STABILITY ANALYSIS

Specification of f_i/f_s

The comparison of the experimental results with stability theory depends critically on the specification of f_i/f_s or of δ and β defined in Eq. 51. Miya (1970) made measurements of f_i as a function of liquid Reynolds number for an air-water flow for different gas velocities. Values of δ and β calculated from the slopes of these curves just prior to the initiation of roll waves are summarized in Table 1. It is noted that β is approximately constant at high gas velocities and decreases rather rapidly at gas Reynolds numbers lower than about 24,000.

Measurements of δ and β were made by Andreussi at high Re_g when the data shown in Figure 3 were taken. These are described reasonably well by Eq. 49 (Figure 2). No systematic variation of β and δ with liquid viscosity was found, when plotted in this manner. Andreussi's measurements of δ and β are compared with those obtained by Miya in Table 1. It is noted that there is some disagreement.

For the comparison of stability theory and with experiment, we have chosen to use the Miya measurements for $Re_g < 24{,}000$ and the Andreussi measurements at larger Re_g.

Comparison with Pseudosteady-State Analysis

Calculations of the stability conditions for air and water from Eqs. 56 and 59 for $\gamma_i = 0$ are shown in Figure 6. Good agreement between this calculation and experiment is obtained at high liquid Reynolds numbers. However, for low liquid Reynolds number, the film is more stable than what is calculated.

Comparison with an Analysis Using a Relaxed Interfacial Stress

A comparison of the effect of liquid viscosity on the critical liquid Reynolds number at a high gas velocity ($Re_g = 40{,}000$) with Eq. 64 is given in Figure 3. It is noted that the transition can be explained if it is assumed that the relaxation of the interfacial stress can be represented by Eq. 44 with $\gamma_i = 27$. The wavelength of the small ripples is approximately 25 times the film height. Therefore, this interpretation would indicate a relaxation length, m_{Li}, which is equal to one ripple length.

A comparison of stability criterion (Eq. 59), using $\gamma_i = 27$, with observations for an air-water flow is given in Figure 6.

DISCUSSION

The agreement between linear stability theory and the observed transition at low gas velocities is excellent. Some improvement over the previous calculations of Hershman and Hanratty is obtained by including the effect of film roughness on the interfacial drag.

The use of linear stability theory to explain the transition to roll waves observed at high gas velocities requires that $\hat{\tau}_{i,I}$ and $\hat{\tau}_{w,I}$ be nonzero and stabilizing. This can come about because of a relaxation of τ_i and τ_w from their pseudosteady-state relations.

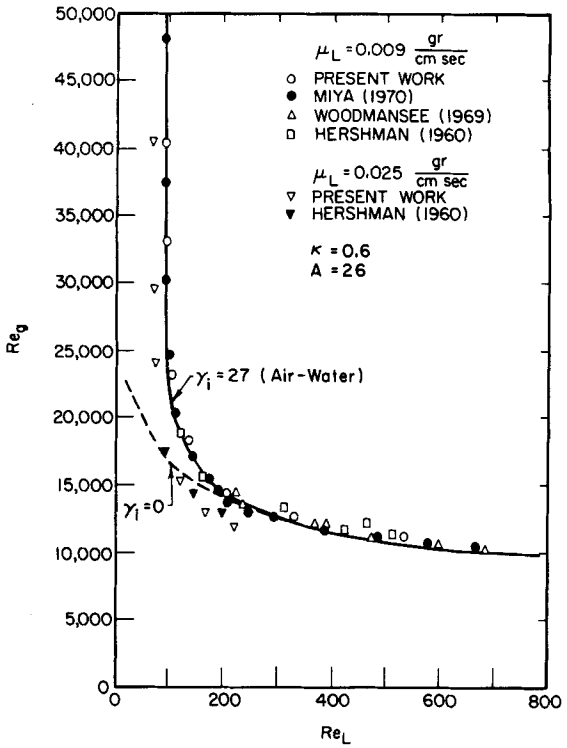

Figure 6. Effect of gas Reynolds number on transition for liquid with viscosities of 0.009 and 0.025 g/cm·s.

Although results are presented only for a relaxed τ_i, we have actually considered both cases. On the basis of such calculations, we have ruled out an explanation based on a relaxed τ_w because it predicts a much stronger dependency of the critical liquid Reynolds number on $\mu_L \rho_g^{1/2} / \mu_g \rho_L^{1/2}$ than is observed.

The absence of roll waves at low liquid Reynolds numbers could occur not only because of the relaxation of interfacial or wall stresses, but also because the rate of growth or the character of the unstable waves are such that they cannot be observed. A slow growth mechanism does not seem reasonable since, at transition, the roll waves are first observed closed to inlet, rather than close to the outlet. The possibility that the unstable waves are not observable at low Reynolds numbers is more attractive.

It could be argued that the instability is manifested as a very low amplitude swell that does grow to an observable disturbance until it assumes a velocity much larger than the liquid film. According to Eq. 63, large values of $c/\overline{u}_i$ would occur if f_i increases with liquid Reynolds number. The transition would then be explained by a somewhat sudden change in the rate of increase of f_i with increasing Re_L. From Eq. 49, it would be expected that such a transition would occur at an approximately fixed value of h_g^+. This type of criterion is unattractive because it predicts a much stronger dependency of the critical liquid Reynolds number on $\mu_L \rho_g^{1/2} / \mu_g \rho_L^{1/2}$ than is observed.

ACKNOWLEDGMENT

The authors acknowledge financial support from the Shell Oil Co., NSF CPE 72-20980, the NSF U.S.-Italy Cooperative Science Program, and CNR of Italy.

NOTATION

A = function of Re_L defined by Eqs. 25 and 26
A_f = parameter defined by Eq. 57
B = channel height
c = wave velocity
f = function defined by Eq. 20

f_s = friction factor for single-phase flow defined by Eq. 50
f_i = friction factor for gas-liquid flow defined by Eq. 31
g = acceleration of gravity
$g(Re_L)$ = $[(1.414Re_L^{0.5})^{2.5} + (0.132Re_L^{0.9})^{2.5}]^{0.4}$
h = instantaneous film height
H = dimensionless height = $\bar{h}/(B - \bar{h})$
$m_{L,i}$ = lag parameter for interfacial stress
p = pressure in the liquid
p_g = pressure in the gas
P_1 = $d\bar{p}/dx\bar{h}^2/\mu_L\bar{u}_a$
P = $\bar{P}\bar{h}^2/\mu_L\bar{u}_a$
$\tilde{P}$ = $dp/dx - \rho_L g \cos\theta$
Re_L = liquid Reynolds number = hu_a/ν_L
$Re_{L,e}$ = effective Reynolds number defined by Eq. 40
Re_g = gas Reynolds number = $(B - h)U_a/\nu_g$
t = time
T = $\bar{\tau}_i\bar{h}/A\mu_L\bar{u}_a$
u = local liquid velocity
u_i = velocity of the liquid at the interface
U = local gas velocity
u_a = average liquid velocity
U_a = average gas velocity
u^* = $\sqrt{\tau_i/\rho_g}$ = friction velocity
u_c^* = $\sqrt{\tau_c/\rho_L}$ = friction velocity
X = $x - ct$
x = distance in flow direction
y = distance from wall

Greek Letters

α = wave number
β = function of Re_g defined by Eq. 51
δ = function of Re_g defined by Eq. 51
Γ = shape factor for velocity profile defined by Eq. 6
γ_i = lag constant for the interfacial stress defined by Eq. 43
Φ = $\bar{\tau}_B/\bar{\tau}_i$
θ = angle between the direction of flow and gravity
μ = viscosity
ν = kinematic viscosity
ρ = density
σ = surface tension
τ = shear stress
τ_B = shear stress at the top wall of the channel
τ_c = characteristic shear stress defined by Eq. 22
τ_i = shear stress at the interface
τ_w = shear stress at the bottom wall of the channel

Superscripts

$'$ = fluctuating quantity
$\bar{}$ = time averaged quantity
$\hat{}$ = amplitude of fluctuating quantity
$+$ = dimensionless with respect to characteristic velocity and length: for the liquid, $\sqrt{\tau_c/\rho_L}$, $\mu_L/\sqrt{\tau_c\rho_L}$; for the gas, $\sqrt{\tau_i/\rho_g}$, $\mu_g/\sqrt{\tau_i\rho_g}$

Subscripts

g = gas
I = imaginary part of complex quantity
L = liquid
R = real part of complex quantity

LITERATURE CITED

Dressler, R. F., "Mathematical Solution of the Problem of Roll-Waves in Inclined Open Channels," *Comm. on Pure and Appl. Math.*, **2**, 149 (1949).

Dressler, R. F., "Stability of Uniform Flow and Roll Wave Formation," U. S. Natl. Bur. Std., Circ. 521,237 (1952).

Hanratty, T. J., and J. M. Engen, "Interaction Between a Turbulent Air Stream and a Moving Water Surface," *AIChE J.*, **3**, 299 (1957).

Hanratty, T. J., and A. Hershman, "Initiation of Poll Waves," *AIChE J.*, **7**, 488 (1961).

Henstock, W. H., and T. J. Hanratty, "The Interfacial Drag and the Height of the Wall Layer in Annular Flows,"*AIChE J.*, **22**, 990 (1976).

Hershman, A., "The Effect of Liquid Properties on the Interaction Between a Turbulent Air Stream and a Flowing Liquid Film," Ph.D. Thesis, Univ. of Illinois, Urbana (1960).

Ishihara, T., Y. Iwagaki, and Y. Ishihara, "On the Rollwave Trains Appearing in Water Flow on a Steep Slope Surface," *Memoirs of the Faculty of Eng.*, Kyoto Univ., **14**, 81 (1952).

Ishii, T. J., and M. A. Grolmes, "Inception Criteria for Droplet Entrainment in Two-Phase Concurrent Film Flow," **21**, 308 (1975).

Iwasa, Y., "The Criterion for Instability of Steady Uniform Flows in Open Channels," *Memoirs of the Faculty of Eng.*, Kyoto Univ., **16**, 264 (1954).

Jeffreys, H., "The Flow of Water in an Inclined Channel of Rectangular Section," *Phil. Mag.*, *49*(6), 793 (1925).

Kinney, G. R., A. E. Abramson, and J. L. Sloop, "Internal Liquid Film Cooling Experiments with Air Stream Temperature to 2,000°F in 2 and 4 in. Diameter Horizontal Tubes," NACA Rept. 1087 (1957).

Knuth, E. L., "The Mechanics of Film Cooling," Parts I and II, *Jet Propulsion*, **24**, 359 (1954) and **24**, 16 (1955).

Lighthill, M. J., and G. B. Whitham, "On Kinematic Waves I Flood Movement on Long Rivers," *Proc. Ray. Soc.*, **A229**, 281 (1955).

Mayer, P. G., "A Study of Waves and Slug Flows in Inclined Open Channels," Ph.D. Thesis, Cornell Univ. (1957).

Miya, M., "Properties of Roll Waves," Ph.D. Thesis, Univ. of Illinois, Urbana (1970).

Miya, M., D. E. Woodmansee, and T. J. Hanratty, "A Model for Roll Waves in Gas-Liquid Flow," *Chem. Eng. Sci.*, **26**, 1915 (1971).

Nedderman, P. M., and C. J. Shearer, "The Motion and Frequency of Large Disturbance Waves in Annular Two-Phase Flow of Air-Water Mixtures," *Chem. Eng. Sci.*, **18**, 661 (1963).

Nencini, F., and P. Andreussi, "Studies of the Behavior of Disturbance Waves in Annular Two-Phase Flow," *Canad. J. Chem. Eng.* (Aug., 1982).

Woodmansee, D. E., and T. J. Hanratty, "Mechanism for the Removal of Droplets from a Liquid Surface by a Parallel Air Flow," *Chem. Eng. Sci.*, **24**, 299 (1969).

Wurz, D. E., "Flussigkeits-Filmstromung Unter Einwirkung Einer Uberschall-Luftstromung," Report Universitat Karlsruhe, Institut fur Thermische Stromungsmaschinen (Feb., 1977).

Manuscript received November 8, 1982; revision received August 9, and accepted October 4, 1983